JGR Space Physics

RESEARCH ARTICLE
10.1029/2021JA030076

Observations of a Strong Intraseasonal Oscillation in the MLT Region During the 2015/2016 Winter Over Mohe, China

Yun Gong[1,2], Junwei Xue[1,2], Zheng Ma[1,2], Shaodong Zhang[1,2,3,4], Qihou Zhou[5], Chunming Huang[1,2], Kaiming Huang[1,2], and Guozhu Li[6]

[1]School of Electronic Information, Wuhan University, Wuhan, China, [2]Key Laboratory of Geospace Environment and Geodesy, Ministry of Education, Wuhan, China, [3]State Key Laboratory of Information Engineering in Surveying, Mapping and Remote Sensing, Wuhan University, Wuhan, China, [4]Guizhou Normal University, Guiyang, China, [5]Electrical and Computer Engineering Department, Miami University, Oxford, OH, USA, [6]Key Laboratory of Earth and Planetary Physics, Institute of Geology and Geophysics, Chinese Academy of Sciences, Beijing, China

Key Points:

- A strong intraseasonal oscillation (ISO) with a period of 40–60 days is first observed in the mesosphere and lower thermosphere at Mohe
- The ISO observed at Mohe is likely associated with the equatorial Madden-Julian Oscillations in the troposphere
- Strong El Niño and the positive Indian Ocean Dipole indices may contribute to the enhancement of the ISO at MH

Correspondence to:
Y. Gong and S. Zhang,
yun.gong@whu.edu.cn;
zsd@whu.edu.cn

Citation:
Gong, Y., Xue, J., Ma, Z., Zhang, S., Zhou, Q., Huang, C., et al. (2022). Observations of a strong intraseasonal oscillation in the MLT region during the 2015/2016 winter over Mohe, China. *Journal of Geophysical Research: Space Physics*, *127*, e2021JA030076. https://doi.org/10.1029/2021JA030076

Received 24 OCT 2021
Accepted 22 MAY 2022

Abstract Using meteor radar measurements at Mohe (MH, 53.5°N, 122.3°E) and the reanalysis data from 2011 to 2020, the characteristics of intraseasonal oscillations (ISOs) in the mesosphere and lower thermosphere (MLT) region over MH are investigated for the first time. The radar observation shows a prominent ISO with periods of 40–60 days in the zonal wind during the 2015/2016 winter. The observed ISO is the strongest in the oscillation period of 30–60 days during nearly a decade of observation. The ISO amplitude reaches a maximum of 16 m/s at 90 km. The vertical structure indicates that intraseasonal variabilities in the lower mesosphere contribute to the ISO in the MLT region. By bandpassing the zonal wind obtained from the reanalysis data along 122.5°E at 52 km in the Northern Hemisphere with cutoff periods of 40 and 60 days, we show that ISOs in the tropical and mid-latitude mesosphere are related to each other. Our results also indicate that the tropical mesospheric ISO and the tropospheric Madden-Julian Oscillations (MJO) are highly correlated. Our analysis suggests that the MJO in the equatorial troposphere may contribute to the enhancement of the ISO in the MLT region over MH. Additionally, a very strong El Niño during the 2015/2016 winter was accompanied by the positive Indian Ocean Dipole, which confines the active MJO in phases 2–4 for a long time. This may be the reason that in the oscillation period of 30–60 days, the ISO observed at MH is the strongest during almost a decade of observation.

1. Introduction

An intraseasonal oscillation (ISO) refers to an atmospheric oscillation in the period ranging from 20 to 100 days mostly observed in the tropical troposphere. Similar to other dominant large-scale oscillation modes in the atmosphere, such as planetary waves, semiannual oscillations, annual oscillations, and quasi-biennial oscillations, ISOs also have a large impact on the dynamics of the middle atmosphere (e.g., Cheng et al., 2021; Guharay et al., 2012, 2014; Huang et al., 2019; K. Kumar & Jain, 1994; Niranjankumar et al., 2011; Rokade et al., 2012; Sridharan et al., 2007; Vergados et al., 2018; Vincent et al., 1988; Yi et al., 2019; Ziemke & Stanford, 1991).

In the mesosphere and lower thermosphere (MLT) region, ISOs in the zonal wind with periods of ~60 days and 35–40 days were first reported by Eckermann and Vincent (1994) using a medium-frequency (MF) radar at Christmas Island (2°N, 157°W). They suggested that the ISOs in the MLT region are associated with ISO activities in the troposphere. Since then, various mechanisms to explain the existence of ISOs in the MLT region have been extensively investigated (Eckermann et al., 1997; Guharay et al., 2014; Huang et al., 2019; Isoda et al., 2004; K. K. Kumar et al., 2007; Lieberman, 1998; Moss et al., 2016; Rao et al., 2009; Tsuchiya et al., 2016). Many studies suggested that ISOs in the MLT region are induced by the upward propagating gravity waves and tides modulated by the tropospheric convection associated with Madden-Julian Oscillations (MJOs) in the lower atmosphere (Eckermann et al., 1997; Guharay et al., 2014; Isoda et al., 2004; K. K. Kumar et al., 2007; Lieberman, 1998; Tsuchiya et al., 2016; Yi et al., 2019). Miyoshi and Fujiwara (2006) and Forbes et al. (2009) reported that interaction between ultrafast Kelvin waves and diurnal tides could generate ISOs in the MLT region. Ziemke and Stanford (1991) first proposed that ISOs in the tropical troposphere can be refracted to the subtropical areas from where they propagate upward in the stratosphere, and then arch back toward the tropical latitudes and propagate to the stratopause. Using ground-based radars, satellite onboard instruments, and a re-analysis data

set, Niranjankumar et al. (2011) concluded that tropical ISO could propagate upward from the troposphere to the upper mesosphere by partial refraction and reflection processes.

Madden-Julian Oscillations (MJOs) are characterized by large-scale convective anomalies over the equatorial Indian and western/central Pacific oceans with periods from 30 to 90 days. They propagate eastward at an averaged velocity of ∼5 m/s (Zhang, 2005 and references therein). Since Madden and Julian (1971, 1972) first documented a 40- to 50-day oscillation in the zonal wind in the tropical troposphere at Canton Island (3°S, 172°W), numerous observational and numerical studies to investigate the detailed structure, dynamical process, generation mechanisms of MJOs, and their impacts on the atmosphere have been reported (Jiang et al., 2020 and references therein). Detailed reviews of MJOs can be found in Zhang (2005) and Jiang et al. (2020).

While there have been numerous studies on ISOs at equatorial/low latitude regions, the characteristics of ISOs in the MLT region at middle and high latitudes are rarely reported. Using two meteor radars at the UK (52°N, 2°W) and ESRANGE (68°N, 21°E) stations, Pancheva et al. (2003) observed an ISO with a period of ∼75 days in the mean winds in the MLT region. They found that the observed ISO was not associated with gravity waves and tidal activities in the troposphere (Pancheva et al., 2003). Based on measurements from a meteor radar at Beijing (40.3°N, 116.2°E), Huang et al. (2019) observed an ISO with a period of ∼30 days in the MLT region and proposed that the ISO might originate from the polar region.

In the present study, using long term observations from a meteor radar located at Mohe (MH, 53.5°N, 122.3°E), China in conjunction with the Modern-Era Retrospective Analysis for Research and Applications, Version 2 (MERRA2) reanalysis data, we investigate the characteristics of mid-latitude ISOs in the MLT region. Data acquisition and processing methods are described in Section 2. Characteristics of ISOs over MH and possible generation mechanisms are presented and discussed in Section 3. Conclusions are given in Section 4.

2. Data and Methodology

The neutral wind data used in this study is derived from a meteor radar located at Mohe (53.5°N, 122.3°E), China, which is operated by the Institute of Geology and Geophysics, Chinese Academy of Sciences. Detailed descriptions of the meteor radar can be found in Hocking et al. (2001) and Yu et al. (2013). In the present study, the zonal wind from 19 August 2011 to 28 June 2020 in the altitude range from 80 to 96 km is used. The temporal and altitudinal resolutions are 1 hr and 2 km, respectively. The daily mean winds are calculated when at least 75% of the data points are available each day.

To study the dominant ISOs in the MLT region, a wavelet transform is applied and the "Morlet" is chosen as the mother wavelet (Torrence & Compo, 1998). A cubic spline interpolation method is used first to make the daily mean winds evenly spaced in time.

To investigate the generation mechanisms of ISOs in the MLT region at mid-latitudes, the MERRA2 reanalysis data is applied. The MERRA2 data used in this study have a temporal resolution of 1 day, a horizontal resolution of 0.5° × 0.625° (latitude times longitude), and 72 pressure levels covering the altitudinal range of ∼0–∼80 km. Details of the MERRA2 reanalysis data can be found in Molod et al. (2015).

In addition to the meteor radar and the MERRA2 reanalysis data, the Real-time Multivariate MJO indices (RMM1 and RMM2), outgoing long-wave radiation (OLR) data, Multivariate El Niño Southern Oscillation (ENSO) Index (MEI.v2), and Dipole Mode Index (DMI) are used to analyze the tropical MJO, El Niño, and Indian Ocean Dipole (IOD). The RMM indices are obtained via empirical orthogonal functions that combine daily mean fields for zonal winds at 850 hPa and 200 hPa and satellite observed OLR averaged over the tropics (15°S–15°N) to measure the amplitude and phase of MJOs. A detailed description of the RMM indices can be found in Wheeler and Hendon (2004). The OLR data is provided by the National Centers for Environmental Prediction and a detailed description of the data can be found in Liebmann and Smith (1996). The ENSO index is the time series of the leading combined Empirical Orthogonal Function based on five different parameters (sea surface temperature, sea level pressure, zonal surface wind, meridional surface wind, and OLR) over the tropical Pacific basin (30°S–30°N and 100°E–70°W). A detailed description of this index is given by Wolter and Timlin (2011). The DMI is an indicator of the sea surface temperature anomaly between the west (50°E–70°E and 10°S–10°N) and east (90°E–110°E and 10°S–0°N) of the equatorial Indian Ocean (IO). Positive (negative)

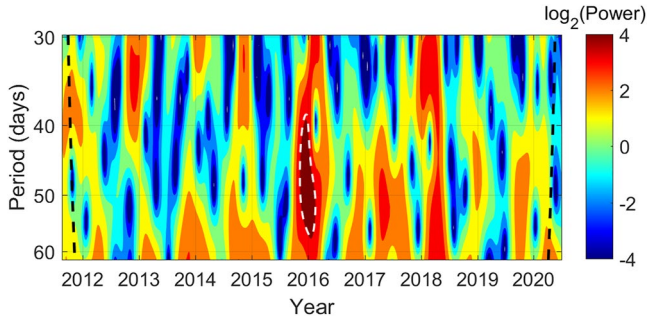

Figure 1. Wavelet spectrum of the daily mean zonal wind obtained from the meteor radar at 90 km from 19 August 2011 to 28 June 2020. The black dashed lines denote the cone of influence for the wavelet analysis and the white dashed line represents a 95% confidence level.

DMI represents a positive (negative) IOD phenomenon. The positive (negative) IOD phenomenon means that the water of the western tropical IO is warmer (cooler) than normal and the water of the eastern tropical IO is cooler (warmer) than normal.

A least-square fitting method is applied to the meteor radar measurements and MERRA2 data to extract the amplitude and phase of the ISO. Since the period of the ISO is not constant, the Lomb-Scargle (LS) spectrum method (Scargle, 1982) is applied to derive the dominant oscillation mode at each altitude. Based on the LS results, the strongest oscillation mode at each altitude is selected as the fitting period of the ISO.

3. Results and Discussions

The result of the wavelet spectrum of the daily mean zonal wind at 90 km in the period from 19 August 2011 to 28 June 2020 is presented in Figure 1. The region of the spectrum within the white dashed curve is above the 95% confidence level. As shown in Figure 1, in the 2015/2016 winter, the spectral value is significant in the period of ~40–60 days, which indicates the existence of a strong ISO. It is of special interest to note that in the oscillation periods ranging from 30 to 60 days, the observed ISO in the winter of 2015/2016 is the strongest during almost a decade of observation in the MLT region at MH.

In Figure 2, we present the least-square fitting results of the ISO amplitude (a) and phase (b) in the altitude range from the surface to 96 km over MH in the period from 1 October 2015 to 31 January 2016. As mentioned in Section 2, the fitting period of the ISO at each altitude is based on the LS results. The vertical profile of the fitted periods of the ISO is presented in Figure 2c. In Figure 2, the red curves represent the results derived from the meteor radar measurements, and the results obtained from the MERRA2 data are presented by the blue curves. By comparing the wind measurements from the Christmas Island MF radar and the Kototabang meteor radar, Venkateswara Rao et al. (2012) found that the difference of the mean wind obtained from the two radars is 2.4 m/s and 1.5 m/s for the zonal and meridional components, respectively. Franke et al. (2005) reported that the root-mean-square wind difference between a meteor radar and a sodium (Na) Doppler lidar is in the range of

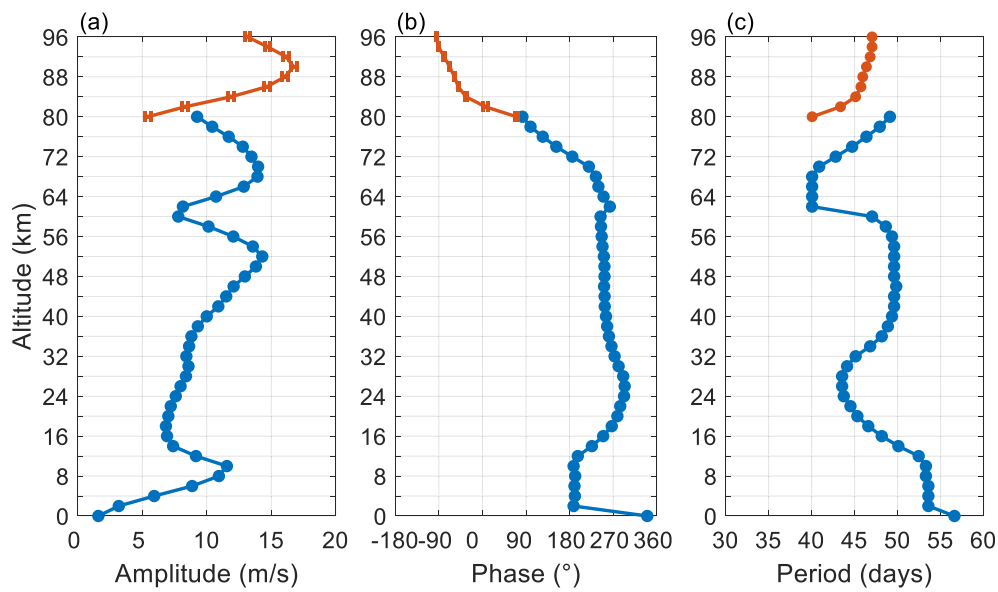

Figure 2. The variations of the intraseasonal oscillation (a) amplitude, (b) phase, and (c) fitted period in the daily mean zonal wind in the period from 1 October 2015 to 31 January 2016 over MH. The red line is derived from meteor radar measurements and the blue line is obtained from the Modern-Era Retrospective Analysis for Research and Applications, Version 2 reanalysis data. The error bars represent the range of one standard deviation estimated using Monte Carlo simulations.

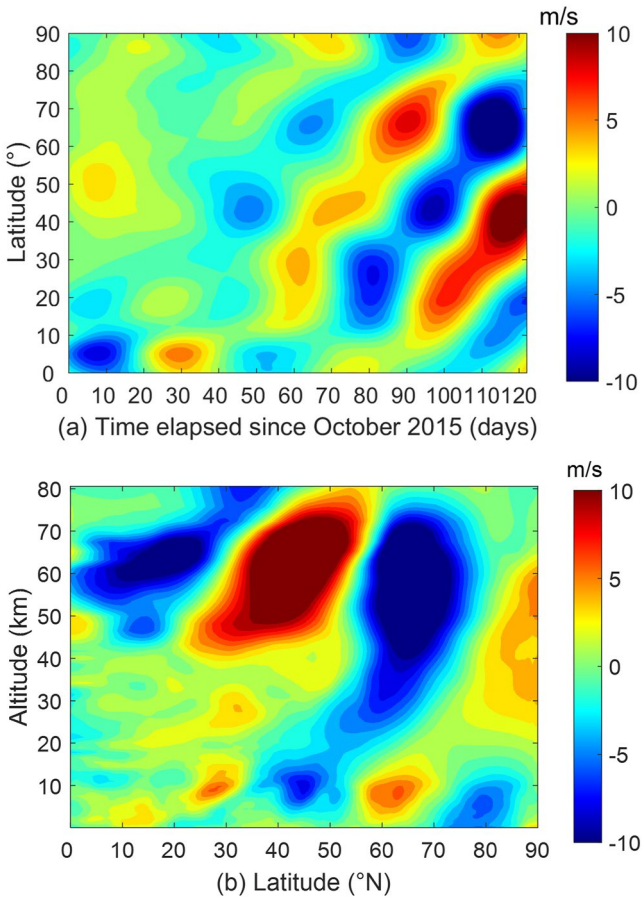

Figure 3. (a) The temporal and latitudinal variations of the filtered daily mean zonal winds within the band of 40–60 days from 1 October 2015 to 31 January 2016 at an altitude of 52 km and a longitude of 122.5°E; (b) The height and latitude distribution of the filtered daily mean zonal winds within the band of 40–60 days on day 115 at a longitude of 122.5°E.

12–17 m/s at altitudes between 80 and 96 km. In the present study, we select 12 m/s as the level of measurement uncertainty of the neutral winds. The fitting error is estimated using Monte Carlo simulations, which is presented as error bars in Figure 2. As shown in Figure 2a, the vertical variation of the ISO amplitude exhibits four peaks at ~90, 70, 52, and 10 km with magnitudes of ~16, 13, 14, and 11 m/s, respectively. The ISO phase shows a clear downward progression above ~60 km. In general, the amplitude of atmospheric waves increases as they propagate upward due to lesser density at higher altitudes. However, the ISO amplitude exhibits a steady decrease in the altitude range from 68 to 80 km, indicating energy dissipation in this region. In the altitude range from ~24 to 60 km, the ISO phase exhibits limited variation. Below 24 km, the ISO phase first decreases with decreasing altitudes and then becomes constant, indicating downward ISO propagation. Thus, the peak amplitude at around 10 km may not be associated with the peak in the MLT region. The characteristics in Figure 2 suggest that ISO variabilities in the lower mesosphere may contribute to the observed ISO in the upper MLT region.

Since ISOs usually prevail in the tropics, it is possible that the ISO observed at MH is linked with ISO variability in the equatorial/low latitude region. To investigate any possible linkage, bandpass filters with cutoff periods of 40 and 60 days are applied to the MERRA2 daily mean zonal winds along 122.5°E longitude in the Northern Hemisphere. Figure 3a presents the temporal and latitudinal distribution of the filtered daily mean zonal wind at 52 km from 1 October 2015 to 31 January 2016. As seen from Figure 3a, in the lower mesosphere, it appears that an ISO with periods from ~40 to 60 days exists from the tropics to high latitudes. The structure shown in Figure 3a indicates that ISO propagates from low to high latitudes. Figure 3b shows the height-latitude distribution of the filtered daily mean wind on day 115. According to Figure 3b, it appears that the poleward propagation of the ISO started in the mesosphere. As mentioned in the introduction, many studies suggest that tropical ISOs in the MLT region are associated with MJO activities in the troposphere (Eckermann et al., 1997; Isoda et al., 2004; Lieberman, 1998). It may be possible that the mesospheric ISO in the tropics is associated with MJO activities in the troposphere.

To investigate the possible association between the ISO in the equatorial mesosphere and the MJO in the troposphere, the MJO activity during the winter of 2015/2016 is examined first. Figure 4 presents the phase-space diagram of MJO indices (RMM1 and RMM2) in the period from 1 October 2015 to 31 January 2016. The state of the MJO is represented by points (green in October, orange in November, blue in December, and red in January), which are determined by RMM1 and RMM2 (Wheeler & Hendon, 2004). The RMM indices delineate the strength, position, and propagating direction of the MJO. When a point is farther away from the central circle, the MJO is stronger. The MJO is too weak to discern using the RMM methods if a point is inside the central circle. The RMM phase diagram is divided into eight equal sectors that coincide with locations of MJO-convection along the equator around the globe (phases 2 & 3: IO, phases 4 & 5: Maritime Continent, phases 6 & 7: western Pacific, phases 8 & 1: western hemisphere and Africa). In Figure 4, the numbers near the points correspond to the dates. Based on the numbers, the propagating direction of the MJO can be revealed. As shown in Figure 4, in the period from October 23 to 22 December 2016, the MJO index travels back and forth from phases 2 to 5. During this period, the RMM1 and RMM2 indices are outside the central circle for 46 days, which indicates an active and long-lasting MJO exists in phases 2 to 5. Note that the longitude of MH is within the Maritime Continent (Phase 4). After that, the points move anticlockwise, which means that the MJO-convection propagates eastward along the equator. Note that the horizontal phase speed of the MJO in phases 2 to 5 is slower than it in other phases (6, 7, 8, and 1). The higher horizontal phase speed at the other phases may form a favorable condition for the MJO propagating upward. However, the characteristics of the MJO at other phases are beyond the scope of the current paper. To investigate the MJO signature in the tropical convection, we perform an LS analysis of the OLR data

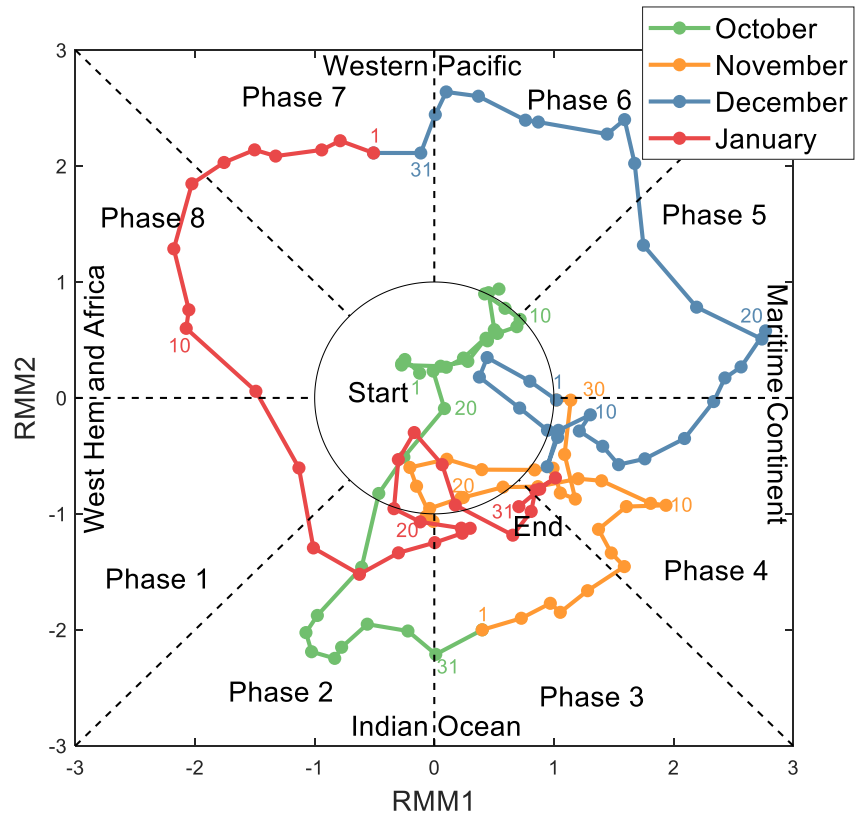

Figure 4. The Phase-space diagram of Madden-Julian Oscillation indices (RMM1 and RMM2) in eight equal sectors (phases 2 & 3: Indian Ocean, phases 4 & 5: Maritime Continent, phases 6 & 7: western Pacific, phases 8 & 1: western hemisphere and Africa) in the period from 1 October 2015 to 31 January 2016. The green, orange, blue, and red curves represent the results in October 2015, November 2015, December 2015, and January 2016, respectively.

along 122.5°E longitude in the latitude range of 5°S–5°N from 1 October 2015 to 31 January 2016 and present in Figure 5. The spectral result indicates a strong MJO signature with a period of ~45 days in the OLR data.

The strong MJO leads us to evaluate the association between the troposphere MJO and the mesospheric ISO. Like gravity waves, when the zonal phase velocity of ISO is smaller than the mean flow, it encounters a critical layer and cannot propagate upward to the MLT region (e.g., Eckermann & Vincent, 1994; Eckermann et al., 1997; Isoda et al., 2004; Rao et al., 2009; Zhou & Morton, 2007). Using the MERRA2 data, we examine the vertical variation of the amplitude and phase of the ISO and find that the ISO cannot directly propagate upward from the troposphere to the lower mesosphere. We also examine the cross-correlation between the ISO in the equatorial mesosphere and the MJO in the troposphere, and between the ISO in the MLT region over MH and the MJO in the equatorial troposphere. The zonal wind obtained from the MERRA2 data in the latitudinal range of 0°N–5°N and at longitude 122.5°E is averaged first. Then, the averaged zonal wind obtained from the MERRA2 data and zonal wind measured from the meteor radar at 92 km over MH are passed through a bandpass filter with cutoff periods of 40 and 60 days. Figure 6 shows the results of (a) the filtered zonal wind at 14 (orange), 52 (red), and 92 (blue) km and (b) the cross-correlation coefficients between zonal wind at 14 and 52 km (blue), and 92 and 14 km (red). As seen from Figure 6a, the filtered zonal wind at 14 km (blue) has a periodic variation with a period of ~50 days and its magnitude largely varies from −6 to 6 m/s, which is a clear MJO signature. The magnitude of the filtered zonal wind at 52 km is generally smaller than at 14 km. Note that the period of the ISO at 14 km is slightly larger than that at 52 km, which might be due to the effect of the background

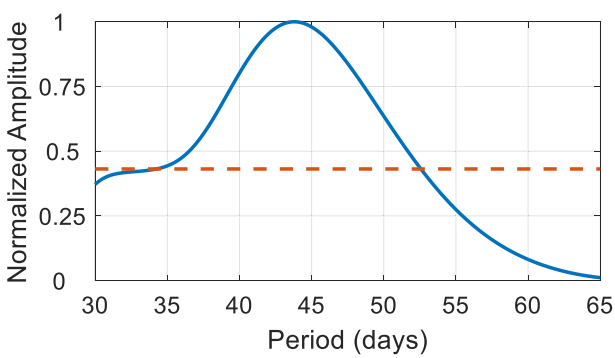

Figure 5. Normalized Lomb-Scargle periodogram of the outgoing long-wave radiation data from 1 October 2015 to 31 January 2016 at the latitude range from 5°S to 5°N and longitude of 122.5°E. The red dashed line indicates the 95% confidence level.

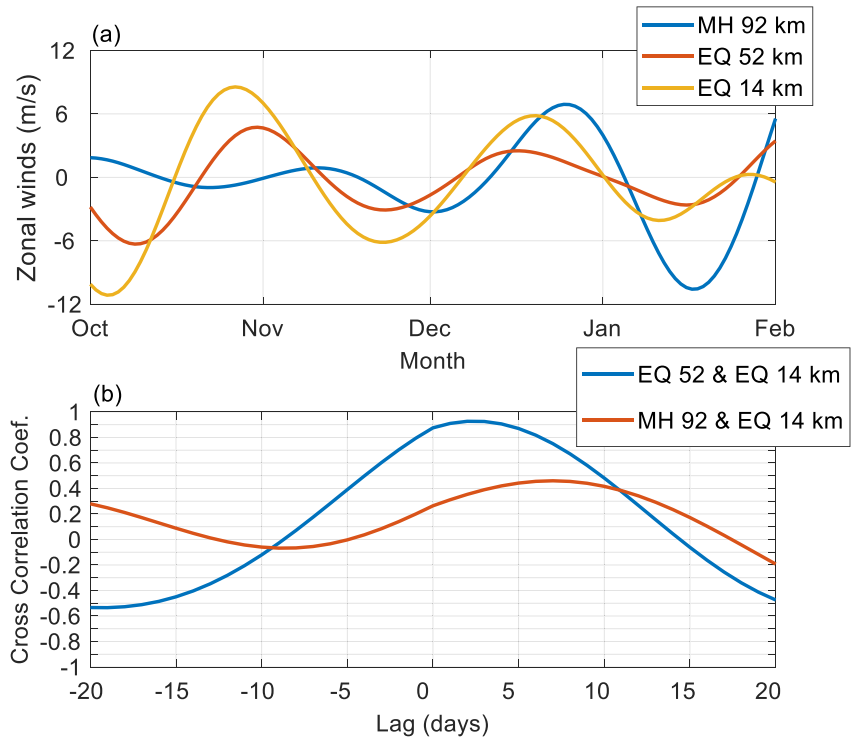

Figure 6. The variations of the filtered daily mean zonal winds (a) averaged in the latitudinal range of 0°N–5°N at 122.5°E at 52 km (red) and 14 km (orange), and the filtered zonal wind at 92 km (blue) over MH within the passband of 40–60 days from 1 October 2015 to 1 February 2016 and (b) the cross-correlation coefficient of filtered daily mean zonal winds at 52 and 14 km (blue), and 92 and 14 km (red).

wind. According to Figure 6b, the maximum cross-correlation coefficient between the MJO in the troposphere and the ISO in the equatorial mesosphere is 0.9 with a time lag of 2 days, indicating that the equatorial ISO in the mesosphere and the MJO in the troposphere are highly correlated and the phase of the tropospheric MJO is ahead of the mesospheric ISO. Unlike the high correlation in the equatorial region, the maximum cross-correlation coefficient between the ISO in the MLT region over MH and the MJO in the troposphere decreased to 0.5 with a time lag of 7 days. A possible reason for the smaller cross-correlation coefficient between the ISO in the MLT region and the MJO in the troposphere is that the MJO signal is modulated by the background atmosphere and atmospheric waves as it travels from the equatorial troposphere to the mid-latitude MLT region.

As mentioned in the introduction, two generating mechanisms of ISOs in the MLT regions are accepted in general. One is that ISOs in the MLT region are induced by the upward propagating gravity waves and tides which are modulated by the tropospheric convection associated with MJOs in the lower atmosphere (Eckermann et al., 1997; Guharay et al., 2014; Isoda et al., 2004; Rao et al., 2009; Tsuchiya et al., 2016). The other is that ISOs in the troposphere at tropical latitudes can be refracted to the subtropical latitudes from where they propagate upward into the stratosphere, and then arch back toward the tropical latitudes and propagate to the mesospheric region (Niranjankumar et al., 2011; Ziemke & Stanford, 1991). It may be possible that the MJO signal was carried by either of these two mechanisms upward from the troposphere to the mesosphere and then the intraseasonal variability propagates poleward to higher latitudes. Our analysis suggests that the active MJO may contribute to the enhancement of the ISO observed at MH.

ISOs are rarely reported in the MLT region at middle and high latitudes. Why is the ISO with periods from 30 to 60 days strongest in the 2015/16 winter during almost a decade of observation over MH? One possible reason is the effect of the interaction between the active MJO and strong El Niño during the 2015/2016 winter. The ENSO (a) and IOD (b) indices in the period from 2011 to 2020 are presented in Figure 7. As shown in Figure 7a, from October 2015 to January 2016, the ENSO index is positive and larger than 0.5 most of the time, which means a very strong El Niño prevailing over the equatorial Pacific. Meanwhile, according to Figure 7b, the IOD index is positive, which means that considerable warming occurs in the western IO. Under the influences of the strong

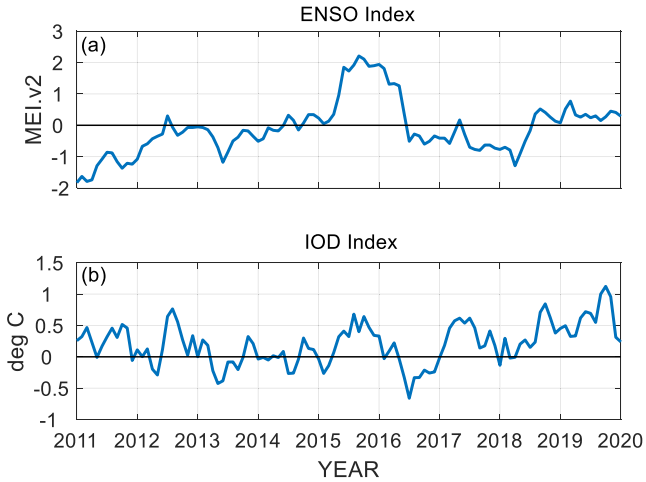

Figure 7. The variations of the (a) El Niño Southern Oscillation index and (b) Indian Ocean Dipole index from January 2011 to January 2020.

El Niño and positive IOD, strong easterlies induced by the El Niño and the eastward-moving MJO caused by the positive IOD interact with each other during the 2015/2016 winter. The strong easterlies may hinder the MJO from propagating eastward and confine the MJO within phases 2–4 (Geetha & Balachandran, 2021; Sreekala et al., 2018). Note that the longitude of Mohe (122.3°E) is within Phase 4 of the MJO. Thus, it may be possible that the long-lasting MJO within phases 2–4 contributes to the enhancement of the ISO in the MLT region over MH.

During the winter of 2015–2016, anomalous changes of a quasi-biennial oscillation (QBO) in the zonal wind occurred, which was the first disruption of the QBO propagation since 1953 (e.g., Bai et al., 2021 and references therein). This anomalous event might contribute to the enhancement of the ISO in the MLT region over MH since the 2015/2016 QBO caused a large atmospheric perturbation in the tropical stratosphere (e.g., Diallo et al., 2018). However, a second disruption of the QBO propagation occurred in the winter of 2019–2020 (e.g., Kang & Chun, 2021), and no strong ISO activity was found at MH during that time. Further investigations are needed in order to reveal the potential relationship between the disrupted QBO and ISO activities at MH.

4. Summary and Conclusion

Using the meteor radar measurements at Mohe (MH, 53.5°N, 122.3°E) and MERRA2 reanalysis data in the period from 2011 to 2020, the characteristics of ISOs in the MLT region at middle latitudes are investigated. Wavelet analysis of the zonal wind in the MLT region reveals an intensive ISO with periods of 40–60 days during the 2015/2016 winter. In the oscillation period of 30–60 days, the observed ISO is the strongest during almost a decade of observation over MH. The ISO reaches a maximum of 16 m/s at 90 km. The phase of the ISO exhibits downward progression in the MLT region.

Since ISOs are frequently observed in the tropics, it may be possible that the ISO activities in the tropics contribute to the amplification of the ISO observed at MH. To investigate this possibility, the zonal wind along 122.5°E longitude at 52 km in the Northern Hemisphere is passed through a bandpass filter with cutoff periods of 40 and 60 days. The result indicates that in the mesosphere, the ISO over MH is associated with intraseasonal variabilities in the equatorial region. Previous studies suggest that tropical ISOs in the mesosphere are associated with MJOs in the troposphere. Based on the result of the phase-space diagram of MJO indices from 1 October 2015 to 31 January 2016, the MJO during 2015/2016 winter is very active. The temporal variation of the filtered zonal wind at 52 km using the same bandwidth has the same trend as at 14 km. The result of the cross-correlation indicates that the tropospheric MJO is highly correlated with the mesospheric ISO. Our analysis suggests that the MJO activity in the troposphere in the equatorial region contributes to the enhancement of the strong ISO observed at MH.

The ENSO index from October 2015 to January 2016 is larger than 0.5 most of the time, which indicates the occurrence of a very strong El Niño. During the same period, the largely positive IOD index indicates an eastward-moving MJO. The effects of the strong El Niño and positive IOD may result in the MJO being locked in phases 2 to 4. This may be one of the reasons that in the oscillation period of 30–60 days, the observed ISO at MH in the MLT region during the 2015/2016 winter is the strongest within the span from 2011 to 2020. Nevertheless, numerical simulations are needed to further investigate the generation mechanisms of ISOs in the MLT region in the middle and high latitudes.

Data Availability Statement

The meteor radar data can be downloaded through the Data Center for Geophysics, National Earth System Science Data Sharing Infrastructure (http://wdc.geophys.cn/dbList.asp?dType=MetPublish). The Modern-Era Retrospective Analysis for Research and Applications, Version 2 data are available from the Goddard Earth

Sciences Data and Information Services Center via https://disc.gsfc.nasa.gov/datasets/M2I3NVASM_5.12.4/summary. The RMM indices data is obtained from the website http://www.bom.gov.au/climate/mjo/. The El Niño Southern Oscillation index is obtained from the website https://psl.noaa.gov/enso/mei/. The Dipole Mode Index is obtained from the website https://psl.noaa.gov/gcos_wgsp/Timeseries/DMI/. The outgoing long-wave radiation data is provided by the NOAA/OAR/ESRL PSL, Boulder, Colorado, USA, from their Website at https://psl.noaa.gov/data/gridded/data.interp_OLR.html.

Acknowledgments
We acknowledge the Chinese Meridian Project and BNOSE, IGGCAS for providing the meteor radar data. We also acknowledge the Goddard Earth Sciences Data and Information Services Center for providing the Modern-Era Retrospective Analysis for Research and Applications, Version 2 data. The study is supported by the National Natural Science Foundation of China (through grants 41574142, 42127805, and 42104145), and the U.S. National Science Foundation grant AGS- 2152109.

References

Bai, X. Y., Huang, K. M., Zhang, S. D., Huang, C. M., & Gong, Y. (2021). Anomalous changes of temperature and ozone QBOs in 2015−2017 from radiosonde observation and MERRA-2 reanalysis. *Earth Planetary Physics*, *5*(3), 1–10. https://doi.org/10.26464/epp2021028

Cheng, H., Huang, K., Liu, A. Z., Zhang, S., Huang, C., & Gong, Y. (2021). A quasi-27-day oscillation activity from the troposphere to the mesosphere and lower thermosphere at low latitudes. *Earth Planets and Space*, *73*(1), 183. https://doi.org/10.1186/s40623-021-01521-1

Diallo, M., Riese, M., Birner, T., Konopka, P., Muller, R., Hegglin, M. I., et al. (2018). Response of stratospheric water vapor and ozone to the unusual timing of EI Nino and the QBO disruption in 2015–2016. *Atmospheric Chemistry and Physics*, *18*(17), 13055–13073. https://doi.org/10.5194/acp-18-13055-2018

Eckermann, S. D., Rajopadhyaya, D. K., & Vincent, R. A. (1997). Intraseasonal wind variability in the equatorial mesosphere and lower thermosphere: Long-term observations from the central Pacific. *Journal of Atmospheric and Solar-Terrestrial Physics*, *59*(6), 603–627. https://doi.org/10.1016/S1364-6826(96)00143-5

Eckermann, S. D., & Vincent, R. A. (1994). First observations of intraseasonal oscillations in the equatorial mesosphere and lower thermosphere. *Geophysical Research Letters*, *21*(4), 265–268. https://doi.org/10.1029/93GL02835

Forbes, J. M., Zhang, X., Palo, S. E., Russell, J., Mertens, C. J., & Mlynczak, M. (2009). Kelvin waves in stratosphere, mesosphere and lower thermosphere temperatures as observed by TIMED/SABER during 2002–2006. *Earth Planets and Space*, *61*(4), 447–453. https://doi.org/10.1186/bf03353161

Franke, S. J., Chu, X., Liu, A. Z., & Hocking, W. K. (2005). Comparison of meteor radar and Na Doppler lidar measurements of winds in the mesopause region above Maui, Hawaii. *Journal of Geophysical Research*, *110*(D9), D09S02. https://doi.org/10.1029/2003JD004486

Geetha, B., & Balachandran, S. (2021). Diagnostic analysis of two dos-à-dos extreme northeast monsoon seasons with dipolar rainfall performance. *Theoretical and Applied Climatology*, *144*(1–2), 675–690. https://doi.org/10.1007/s00704-021-03528-w

Guharay, A., Batista, P. P., Clemesha, B. R., Sarkhel, S., & Buriti, R. A. (2014). Investigation of the intraseasonal oscillations over a Brazilian equatorial station: A case study. *Earth Planets and Space*, *66*(1), 145. https://doi.org/10.1186/s40623-014-0145-3

Guharay, A., Sekar, R., Venkat Ratnam, M., & Batista, P. P. (2012). Characteristics of the intraseasonal oscillations in the lower and middle atmosphere over Gadanki. *Journal of Atmospheric and Solar-Terrestrial Physics*, *77*, 167–173. https://doi.org/10.1016/j.jastp.2011.12.016

Hocking, W., Fuller, B., & Vandepeer, B. (2001). Real-time determination of meteor-related parameters utilizing modern digital technology. *Journal of Atmospheric and Solar-Terrestrial Physics*, *63*(2-3), 155–169. https://doi.org/10.1016/S1364-6826(00)00138-3

Huang, K. M., Xi, Y., Wang, R., Zhang, S. D., Huang, C. M., Gong, Y., & Cheng, H. (2019). Signature of a quasi 30-day oscillation at midlatitude based on wind observations from MST radar and meteor radar. *Journal of Geophysical Research: Atmospheres*, *124*(21), 11266–11280. https://doi.org/10.1029/2019JD031170

Isoda, F., Tsuda, T., Nakamura, T., Vincent, R. A., Reid, I. M., Achmad, E., et al. (2004). Intraseasonal oscillations of the zonal wind near the mesopause observed with medium-frequency and meteor radars in the tropics. *Journal of Geophysical Research*, *109*(D21), D21108. https://doi.org/10.1029/2003JD003378

Jiang, X., Adames, Á. F., Kim, D., Maloney, E. D., Lin, H., Kim, H., et al. (2020). Fifty years of research on the Madden-Julian Oscillation: Recent progress, challenges, and perspectives. *Journal of Geophysical Research: Atmospheres*, *125*(17), e2019JD030911. https://doi.org/10.1029/2019jd030911

Kang, M. J., & Chun, H. Y. (2021). Contributions of equatorial planetary waves and small-scale convective gravity waves to the 2019/20 QBO disruption. *Atmospheric Chemistry and Physics*, *21*(12), 9839–9857. https://doi.org/10.5194/acp-21-9839-2021

Kumar, K., & Jain, A. R. (1994). Latitudinal variations of 30–70 day period waves over the tropical Indian zone. *Journal of Atmospheric and Terrestrial Physics*, *56*(9), 1135–1145. https://doi.org/10.1016/0021-9169(94)90052-3

Kumar, K. K., Antonita, T. M., Ramkumar, G., Deepa, V., Gurubaran, S., & Rajaram, R. (2007). On the tropospheric origin of Mesosphere Lower Thermosphere region intraseasonal wind variability. *Journal of Geophysical Research*, *112*(D7), D07109. https://doi.org/10.1029/2006JD007962

Lieberman, R. S. (1998). Intraseasonal variability of high-resolution Doppler imager winds in equatorial mesosphere and lower thermosphere. *Journal of Geophysical Research*, *103*(D10), 11221–11228. https://doi.org/10.1029/98JD00532

Liebmann, B., & Smith, C. A. (1996). Description of a complete (interpolated) outgoing longwave radiation dataset. *Bulletin of the American Meteorological Society*, *77*, 1275–1277. https://doi.org/10.1175/1520-0477(1996)077<1255:EA>2.0.CO;2

Madden, R. A., & Julian, P. R. (1971). Detection of a 40-50 day oscillation in the zonal wind in the tropical Pacific. *Journal of the Atmospheric Sciences*, *28*(5), 702–708. https://doi.org/10.1175/1520-0469(1971)028<0702:DOADOI>2.0.CO;2

Madden, R. A., & Julian, P. R. (1972). Description of global-scale circulation cells in the tropics with a 40-50 Day period. *Journal of the Atmospheric Sciences*, *29*(6), 1109–1123. https://doi.org/10.1175/1520-0469(1972)029<1109:DOGSCC>2.0.CO;2

Miyoshi, Y., & Fujiwara, H. (2006). Excitation mechanism of intraseasonal oscillation in the equatorial mesosphere and lower thermosphere. *Journal of Geophysical Research*, *111*(D14), D14108. https://doi.org/10.1029/2005JD006993

Molod, A., Takacs, L., Suarez, M., & Bacmeister, J. (2015). Development of the GEOS-5 atmospheric general circulation model: Evolution from MERRA to MERRA2. *Geoscientific Model Development*, *8*(5), 1339–1356. https://doi.org/10.5194/gmd-8-1339-2015

Moss, A. C., Wright, C. J., & Mitchell, N. J. (2016). Does the Madden-Julian Oscillation modulate stratospheric gravity waves? *Geophysical Research Letters*, *43*(8), 3973–3981. https://doi.org/10.1002/2016GL068498

Niranjankumar, K., Ramkumar, T. K., & Krishnaiah, M. (2011). Vertical and lateral propagation characteristics of intraseasonal oscillation from the tropical lower troposphere to upper mesosphere. *Journal of Geophysical Research*, *116*(D21), D21112. https://doi.org/10.1029/2010JD015283

Pancheva, D., Mitchell, N. J., Younger, P. T., & Muller, H. G. (2003). Intraseasonal oscillations observed in the MLT region above UK (52°N, 2°W) and ESRANGE (68°N, 21°E). *Geophysical Research Letters*, *30*(21), 2084. https://doi.org/10.1029/2003GL017809

Rao, R. K., Gurubaran, S., Sathishkumar, S., Sridharan, S., Nakamura, T., Tsuda, T., et al. (2009). Longitudinal variability in intraseasonal oscillation in the tropical mesosphere and lower thermosphere region. *Journal of Geophysical Research*, *114*(D19), D19110. https://doi.org/10.1029/2009JD011811

Rokade, M. V., Kondala Rao, R., Nikte, S. S., Ghodpage, R. N., Patil, P. T., Sharma, A. K., & Gurubaran, S. (2012). Intraseasonal oscillation (ISO) in the MLT zonal wind over Kolhapur (16.8°N) and Tirunelveli (8.7°N). *Annales Geophysicae*, *30*(12), 1623–1631. https://doi.org/10.5194/angeo-30-1623-2012

Scargle, J. D. (1982). Studies in astronomical time series analysis, II. Statistical aspects of spectral analysis of unevenly spaced data. *The Astrophysical Journal*, *263*, 835–853. https://doi.org/10.1086/160554

Sreekala, P. P., Rao, S. V. B., Rajeevan, K., & Arunachalam, M. S. (2018). Combined effect of MJO, ENSO and IOD on the intraseasonal variability of northeast monsoon rainfall over south peninsular India. *Climate Dynamics*, *51*(9–10), 9–10. https://doi.org/10.1016/j.atmosres.2019.03.021

Sridharan, S., Tsuda, T., & Gurubaran, S. (2007). Radar observations of long-term variability of mesosphere and lower thermosphere winds over Tirunelveli (8.7°N, 77.8°E). *Journal of Geophysical Research*, *112*(D23), D23105. https://doi.org/10.1029/2007JD008669

Torrence, C., & Compo, G. P. (1998). A practical guide to wavelet analysis. *Bulletin of the American Meteorological Society*, *79*(1), 61–78. https://doi.org/10.1175/1520-0477(1998)079<0061:APGTWA>2.0.CO;2

Tsuchiya, C., Sato, K., Alexander, M. J., & Hoffmann, L. (2016). MJO-related intraseasonal variation of gravity waves in the Southern Hemisphere tropical stratosphere revealed by high-resolution AIRS observations. *Journal of Geophysical Research: Atmospheres*, *121*(13), 7641–7651. https://doi.org/10.1002/2015JD024463

Venkateswara Rao, N., Tsuda, T., Riggin, D. M., Gurubaran, S., Reid, I. M., & Vincent, R. A. (2012). Long-term variability of mean winds in the mesosphere and lower thermosphere at low latitudes. *Journal of Geophysical Research*, *117*(A10), A10312. https://doi.org/10.1029/2012JA017850

Vergados, P., Liu, G., Mannucci, A. J., & Janches, D. (2018). Equatorial intraseasonal temperature oscillations in the lower thermosphere from SABER. *Geophysical Research Letters*, *45*(20), 10893–10902. https://doi.org/10.1029/2018GL079467

Vincent, R. A., Tsuda, T., & Kato, S. (1988). A comparative-study of mesospheric solar tides observed at Adelaide and Kyoto. *Journal of Geophysical Research*, *93*(D1), 699–708. https://doi.org/10.1029/Jd093id01p00699

Wheeler, M., & Hendon, H. (2004). An all-season real-time multivariate MJO index: Development of an index for monitoring and prediction. *Monthly Weather Review*, *132*(8), 1917–1932. https://doi.org/10.1175/1520-0493(2004)132<1917:AARMMI>2.0.CO;2

Wolter, K., & Timlin, M. S. (2011). El Niño/Southern Oscillation behaviour since 1871 as diagnosed in an extended multivariate ENSO index (MEI.ext). *International Journal of Climatology*, *31*(7), 1074–1087. https://doi.org/10.1002/joc.2336

Yi, W., Xue, X., Chen, J., Chen, T., & Li, N. (2019). Quasi-90-day oscillation observed in the MLT region at low latitudes from the Kunming meteor radar and SABER. *Earth and Planetary Physics*, *3*(2), 136–146. https://doi.org/10.26464/epp2019013

Yu, Y., Wan, W. X., Ning, B. Q., Liu, L. B., Wang, Z. G., Hu, L. H., & Ren, Z. P. (2013). Tidal wind mapping from observations of a meteor radar chain in December 2011. *Journal of Geophysical Research: Space Physics*, *118*(5), 2321–2332. https://doi.org/10.1029/2012JA017976

Zhang, C. (2005). Madden-Julian Oscillation. *Reviews of Geophysics*, *43*(2), RG2003. https://doi.org/10.1029/2004RG000158

Zhou, Q., & Morton, Y. T. (2007). Gravity wave propagation in a nonisothermal atmosphere with height varying background wind. *Geophysical Research Letters*, *34*(23), L23803. https://doi.org/10.1029/2007GL031061

Ziemke, J. R., & Stanford, J. L. (1991). One-to-two month oscillations: Observed high-latitude tropospheric and stratospheric response to tropical forcing. *Journal of the Atmospheric Sciences*, *48*(11), 1336–1347. https://doi.org/10.1175/1520-0469(1991)048<1336:OTTMOO>2.0.CO;2